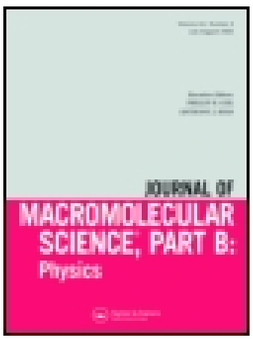

Journal of Macromolecular Science, Part B

ISSN: 0022-2348 (Print) 1525-609X (Online) Journal homepage: https://www.tandfonline.com/loi/lmsb20

Changes in Structural and Optical Properties of Polycarbonate Induced by Ag^+ Ion Implantation

Suman Bahniwal , Annu Sharma , Sanjeev Aggarwal , S. K. Deshpande , Satinder K. Sharma & K. G.M. Nair

To cite this article: Suman Bahniwal , Annu Sharma , Sanjeev Aggarwal , S. K. Deshpande , Satinder K. Sharma & K. G.M. Nair (2010) Changes in Structural and Optical Properties of Polycarbonate Induced by Ag^+ Ion Implantation, Journal of Macromolecular Science, Part B, 49:2, 259-268, DOI: 10.1080/00222340903352252

To link to this article: https://doi.org/10.1080/00222340903352252

Published online: 23 Mar 2010.

Journal of Macromolecular Science®, Part B: Physics, 49:259–268, 2010

ISSN: 0022-2348 print / 1525-609X online
DOI: 10.1080/00222340903352252

Taylor & Francis
Taylor & Francis Group

Changes in Structural and Optical Properties of Polycarbonate Induced by Ag^+ Ion Implantation

SUMAN BAHNIWAL,[1] ANNU SHARMA,[1]
SANJEEV AGGARWAL,[1] S. K. DESHPANDE,[2]
SATINDER K. SHARMA,[3] AND K.G.M. NAIR[4]

[1]Department of Physics, Kurukshetra University, Kurukshetra, India
[2]UGC-DAE Consortium for Scientific Research, Mumbai Centre, Bhabha Atomic Research Centre, Mumbai, India
[3]Nano Science and Nano Technology Unit, Department of Chemical Engineering, I.I.T. Kanpur, India
[4]Material Science Division, Indira Gandhi Centre for Atomic Research, Kalpakkam, India

Transparent polycarbonate samples were implanted with 1 MeV Ag^+ ions to various doses ranging from 5×10^{14} to 3×10^{16} ions cm^{-2} with a beam current density of 900 nA cm^{-2}. Modification in the structure of polycarbonate as a function of the implantation fluence was investigated using micro-Raman spectroscopy, glancing angle X-ray diffraction, and UV-Vis spectroscopy. Raman spectroscopy pointed toward the formation of graphite structures/clusters due to the ion implantation. UV-Vis absorption analysis suggests the formation of a carbonaceous layer and a drastic decrease in optical band gap from 4.12 eV to 0.50 eV at an implanted dose of 3×10^{16} ions cm^{-2}. The correlation between the decrease in band gap and the structural changes is discussed.

Keywords glancing angle X-ray diffraction, optical band gap, polycarbonate, Raman spectroscopy, UV-Vis spectroscopy

Introduction

Ion implantation is a powerful method to modify various properties of polymers,[1] such as optical characteristics,[2–4] conductivity,[5,6] biocompatibility,[7–10] mechanical properties,[2,11–13] etc. The alteration of the polymeric properties is both due to the presence of the implanted impurities, which change the polymer composition, and due to the irradiation-induced effects initiated by them, which alter both the chemical composition and the structure of a polymer by causing chain scission, cross-linking, free radical formation, dangling pair production, etc.[14–16]

Polycarbonate (PC) is widely used in optical applications due to its combination of chemical stability and optical and mechanical properties. It is a potential material for fabrication of optical sensors, light emitting diodes, integrated optics for communication and signal processing, antireflective coatings, etc. Thus, the study of the effect of ion

Received 18 December 2008; accepted 21 May 2009.
Address correspondence to Dr Annu Sharma, Department of Physics, Kurukshetra University, Kurukshetra 136 119, India. E-mail: talk2annu@gmail.com

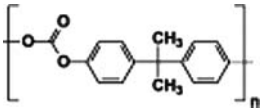

Figure 1. Monomer structure of PC.

implantation on optical properties of PC, such as absorption and band gap, is of immense importance from both fundamental and technological points of view.

The modification of mechanical,[2,12,13,17] and optical properties[17] of PC by gaseous ions has been investigated extensively. Yap et al.[2] examined the effect of Ar and H ions on UV-Vis absorption and mechanical properties of PC. They found that mechanical properties improved as a result of irradiation with both ion species but H implantation produced a yellow-brown material with optical properties similar to amorphous hydrogenated carbon, whereas Ar implantation produced a material with optical properties more like evaporated amorphous carbon. Rodrıguez et al.[12] studied the effect of silicon, nitrogen, deuterium, and hydrogen ion beams on surface mechanical properties of PC. Although their results showed harder surfaces in all cases, except for silicon implantation, the biggest increases in hardness corresponded to hydrogen and deuterium implantation at high fluence. Jinfu San et al.[13] utilized C, Al, Ti, Fe, and Ni ion implantation for improving surface hardness and wear resistance of PC. Radwan et al.[17] studied the effect of He and Ar ion implantation on the optical and electrical properties of PC. They showed that the optical band gap decreases with increasing fluence of both He and Ar ions whereas conductivity increases with increasing fluence of both the ions. In the present study, we expanded the work to include the metallic ion implantation. This work explores the potential improvements in the optical properties of PC by chemically inert silver ions.

The present work examines the effect of silver ion implantation on the structural and optical properties of PC. The chemical and structural changes in PC as a result of implantation were revealed using micro-Raman spectroscopy and glancing angle X-ray diffraction (GXRD). The modification in the absorption and optical band gap of Ag-implanted PC was studied by UV-Vis spectroscopy. The monomer structure of the PC used is shown in Fig. 1.

Experimental

The PC samples of size 2×2 cm^2 were cut from the 250 μm thick, commercially available, and optically transparent sheet. Some of these samples were implanted using a 1 MeV Ag^+ ion beam. The implantation was preformed using an ion flux ranging between 5×10^{14} and 3×10^{16} ions cm^{-2} on the 1.7 MV Tandetron accelerator facility available at Indira Gandhi Centre for Atomic Research, Kalpakkam, India. The beam current density was kept $\sim$900 nA cm^{-2} and the spot size of $\sim$10 mm diameter. During implantation the vacuum inside the chamber was $\sim 10^{-7}$ Torr.

The changes in structure and composition of PC as a result of implantation were examined using a Wi Tec Confocal Micro-Raman Spectrometer (available at IIT Kanpur) with excitation wavelength $\lambda = 532$ nm. To ascertain the changes in the structure of PC, GXRD measurements were carried out using a Seifert 3003TT X-Ray Diffractometer (Cu Kα: $\lambda = 1.5405$ nm) available at UGC-DAE, Consortium for Scientific Research, Mumbai Centre, Bhabha Atomic Research Center, Mumbai, India. The angle of incidence between

the beam and the sample surface was kept at 0.2° in order to characterize the thin surface layer affected, and the diffraction pattern was recorded from 10° to 60° at a scan speed of .2°/minute.

The optical absorption measurements were performed on virgin and implanted samples using a Shimadzu Double Beam Double Monochromator Spectrophotometer (UV-2550), equipped with an Integrating Sphere Assembly ISR-240A in the wavelength range of 190–900 nm with a resolution of 0.5 nm. All the absorption spectra were recorded keeping air as the reference.

Results and Discussion

Micro-Raman spectroscopy is a sensitive technique for probing the local atomic bonding in the implanted samples and hence is a very useful tool to study the microstructural changes in the surface layers of the implanted specimens with a thickness spatial resolution of a few micrometers.

Figure 2 depicts the Raman spectra of pristine and 1 MeV Ag^+-implanted PC samples with various fluence ranging from 5×10^{14} to 3×10^{16} ions cm^{-2}, probed with a 532 nm wavelength beam. For unimplanted PC, the observed frequencies and assignments are summarized in Table 1. The assignments were aided by group frequency considerations.[18–20] The micro-Raman spectrum of PC contains an intense band at 3071 cm^{-1} that can be

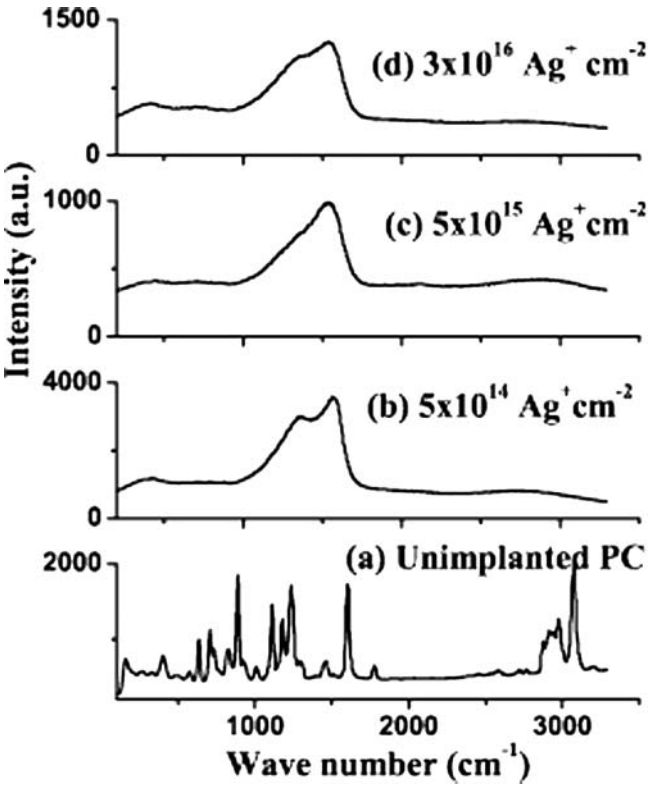

Figure 2. Raman spectra of PC unimplanted (a) and implanted with 1 MeV to a dose of (b) 5×10^{14} Ag^+ cm^{-2}, (c) 5×10^{15} Ag^+ cm^{-2}, and (d) 3×10^{16} Ag^+ cm^{-2}.

Table 1
The assignments of the Raman modes of PC[37–20]

1	3212w	O−H stretch
2	3071s	sp^2 C−H stretch
3	2973m	sp^3 C−H stretch
4	2764w, 2722w, 2587w, 2462w	overtone & combination band
5	1775m	C=O stretch
6	1601s	Ring stretch
7	1517w, 1450m	CH_3 deformation
8	1296sh, 1232s	C−O−C stretch
9	1200s, 1100s	C−O−C stretch, C−H waging (i.p.)
10	1015w	Ring stretch, C−H bend (i.p.)
11	921sh	C−CH_3 stretch, C−H bend (i.p.)
12	880s	C−CH_3 stretch, O−C(O)−O stretch
13	825m	Phenyl ring vibration (o.p.), C−H bend (o.p.)
14	711m	Phenyl ring vibration
15	638m, 565w	Phenyl ring vibration

Note: s, strong intensity; m, medium intensity; w, weak intensity; i.p., in plane; o.p., out of plane.

ascribed to a C−H stretching mode. A series of weak bands in the region 2400–2800 cm^{-1} are attributed to overtone and combination bands. The band at 1780 cm^{-1} is assigned to a C=O stretching mode of PC. At frequencies in the range below 1600 cm^{-1}, a considerable number of bands, largely overlapped, are observed. The bands in this region are associated with stretching of the O−C(O)−O group and modes due to phenyl rings.

After the implantation, the characteristic peaks of PC are completely lost, which suggests that the chemical structure of PC has changed completely. At an implantation dose of 5×10^{14} ions cm^{-2} (Fig. 2b) an asymmetric band, which extends from 900 to 1800 cm^{-1} with two peaks at 1575 cm^{-1} (graphite peak) and 1350 cm^{-1} (disordered peak) became dominant. Such peaks are observed in the first-order Raman spectra of graphite. The relatively sharp, intense peak at 1575 cm^{-1} (G-peak) is assigned to the C−C stretching mode within the graphite basal plane with E_{2g} symmetry, and a disorder peak (D peak) at 1350 cm^{-1} results from the first-order Raman scattering from a zone-edge phonon with A_{1g} symmetry.[21,22] The G peak originates from the ordered hexagon rings consisting of sp^2-bonded carbons and is observed in graphite with large microcrystals,[23] and the D peak in carbon-based materials has been observed for the disordered graphite, such as the clusters of hexagonal rings. In implanted PC samples, an asymmetric band with peak positions at 2800 cm^{-1} is also observed. This broadband at 2800 cm^{-1} is observed in the second-order spectrum of polycrystalline graphite.[22,24] When the dose is further increased to 5×10^{15} ions cm^{-2} (Fig. 2c), G peak becomes broader with only a shoulder at D peak position. At a dose of 3×10^{16} ions cm^{-2}, the D peak starts appearing again (Fig. 2d) and the band at 2800 cm^{-1} disappears.

Thus, as a result of implantation, dehydrogenation occurs and the original peaks of PC are completely lost resulting in the formation of a graphite-like structure. At a dose of the order of 5×10^{14} ions cm^{-2}, a pronounced D peak emerges concurrent with intense G peak, implying that a structural change occurs around a dose of 5×10^{14} ions cm^{-2} from a polymeric material to one which contains a significant fraction of sp^2-bonded material with good in-plane ordering. At a higher dose of 5×10^{15} ions cm^{-2}, both D and G peaks

become broadened and less well-defined, indicating that the increased ion bombardment has decreased the in-plane order within the graphite layer with a simultaneous increase in sp^2 sites.[25] With the further increase in implantation dose, to the order of 3×10^{16} ions cm^{-2}, the intensity of the D and G peaks seems to increase. This can be due to the increasing size and/or increasing number of graphitic clusters.[26,27] The increasing numbers of graphitic clusters hence indicates a rise in the number of clusters of hexagonal rings made up of sp^2-bonded carbons. The high-fluence implantation also leads to the evolution of more hydrogen and transformation from the sp^3 phase of carbon to the sp^2 phase of carbon, considering that high temperature treatment of carbon films containing hydrogen give rise to these consequences.[28] The increase in sp^2 carbon sites is also confirmed by the darkening of the sample.[27] Thus Raman spectroscopy indicates toward the formation of a graphitic network.

Figure 3 shows the GXRD spectra of the pristine and implanted PC. In case of the pristine PC, one broad peak at $2\theta = 17.17^\circ$ has been observed, which indicates the amorphous nature of the polymer. As seen in the figure, the peak area increases with fluence up to an implantation dose of 5×10^{15} ions cm^{-2}. This increase in the peak area indicates some degree of ordering in the carbonaceous layer, which may be due to the oxidation in PC after irradiation.[29,30] When the fluence is further increased to 3×10^{16} ions cm^{-2}, the implantation-induced damage increases; as a result the peak area decreases, indicating some degree of disordering resulting in the formation of carbonaceous network.

The UV-Vis spectrum of pristine and Ag^+-implanted PC with various doses is shown in Fig. 4. Absorption peaks in the UV region are due to electronic transitions between occupied and unoccupied molecular orbitals and the spectrum in this region is particularly sensitive to conjugated bonds. The strongest peaks in the UV are generally due to π–π^* transitions, which are likely to be associated with the phenyl groups in PC.[30] The strong π–π^* peak at 290–300 nm is characteristic of aromatic compounds and is sometimes referred to as the α-peak of the phenyl group. The π–π^* peak is known to shift to higher wavelengths as conjugation is increased. The carbonyl group in PC is also a chromophore

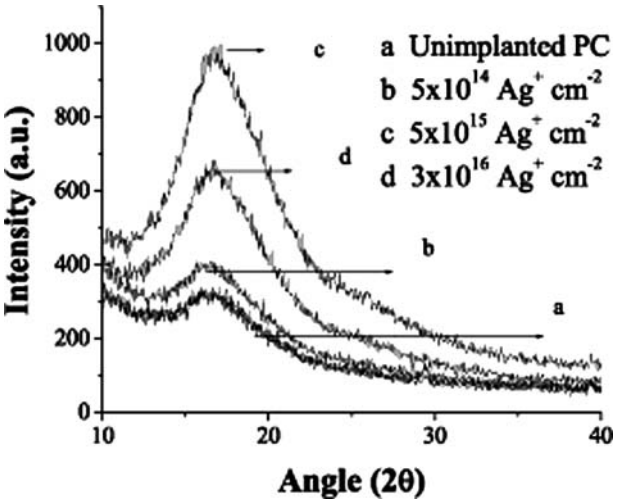

Figure 3. GXRD spectra of PC unimplanted (a) and implanted with 1 MeV to a dose of (b) 5×10^{14} Ag^+ cm^{-2}, (c) 5×10^{15} Ag^+ cm^{-2}, and (d) 3×10^{16} Ag^+ cm^{-2}.

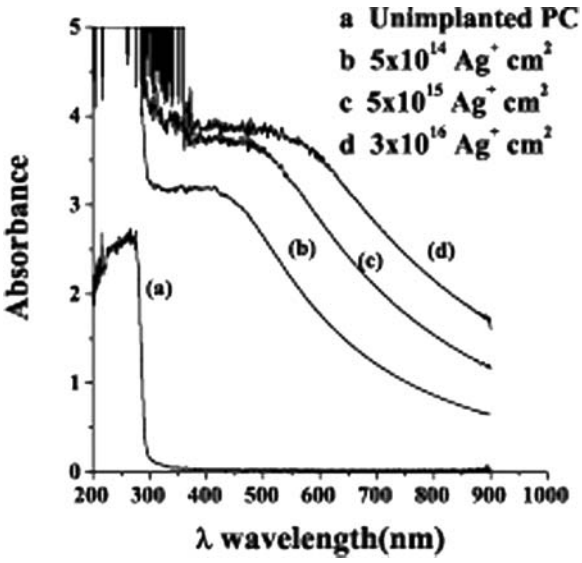

Figure 4. UV-Vis absorption spectra of of PC unimplanted (a) and implanted with 1 MeV to a dose of (b) 5×10^{14} Ag^+ cm^{-2}, (c) 5×10^{15} Ag^+ cm^{-2}, and (d) 3×10^{16} Ag^+ cm^{-2}.

and the absorption peak at 280–290 nm is consistent with the PC carbonyl group n–π^* transitions.[31] From Fig. 4 it is clear that as a result of Ag^+ implantation the absorption increases and the absorption edge shifts to longer wavelengths; the shifting of the onset of absorption to longer wavelength indicates that the band gap energy is reduced as a result of implantation. This has been interpreted as an indicator of the formation of carbonaceous clusters or networks of conjugated unsaturated bonds.

The optical band gap energy (E_g) value of the PC and Ag^+-implanted PC samples were determined from its absorption coefficient (α), obtained from the linear portion of the fundamental absorption edge of the UV-Vis spectra. The absorption coefficient of a material with α of the order of 10^{-5} to 10^{-6} cm^{-1} is related to E_g by the equation $(\alpha h\nu)^{1/2} \sim (h\nu - E_g)$.[32] The E_g value can therefore be obtained by plotting $(\alpha h\nu)^{1/2}$ vs. $h\nu$, and then extrapolating the linear portion of the plot to $(\alpha h\nu)^{1/2} = 0$. Figure 5 shows such plots for pristine PC and Ag^+-implanted PC. The optical band gap energies for pristine PC and Ag^+-implanted PC samples were estimated along with their standard error and results are presented in Table 2. The optical band gap energy of pristine PC was estimated to be 4.12 eV

Table 2
Optical band gap and cluster sizes for the PC samples implanted at different fluence

S. No.	Implanted dose (Ag^+ cm^{-2})	Optical band gap (eV)	No. of carbon atoms
1	Unimplanted	$4.12 \pm .01$	
2	5×10^{14}	$0.81 \pm .03$	1793
3	5×10^{15}	$0.64 \pm .02$	2872
4	3×10^{16}	$0.50 \pm .01$	4706

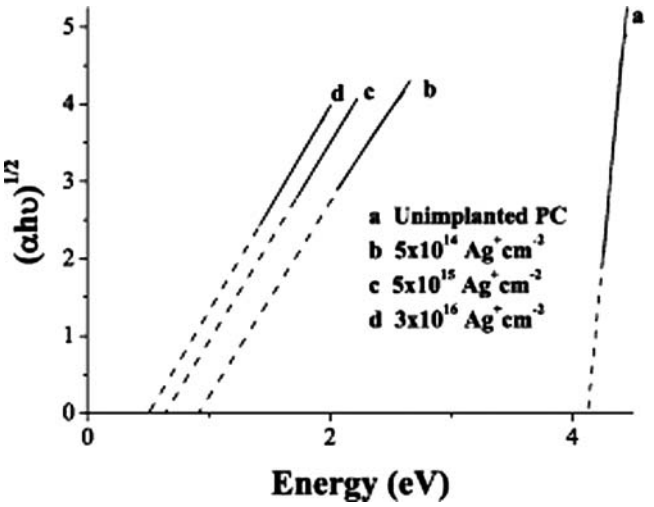

Figure 5. Plots of $(\alpha h\nu)^{1/2}$ vs. energy $(h\nu)$ used to determine optical band gap in PC unimplanted (a) and implanted with 1 MeV to a dose of (b) 5×10^{14} Ag^+ cm^{-2}, (c) 5×10^{15} Ag^+ cm^{-2}, and (d) 3×10^{16} Ag^+ cm^{-2}.

and it drastically declines to a value of 0.50 eV for Ag^+-implanted PC to a dose of 3×10^{16} ions cm^{-2}.

During implantation, hydrogen and other gases are released from polymeric materials, which cause the enrichment of carbon atoms leading to the formation of hydrogenated amorphous carbon.[33] The implantation results in rearrangement and bond shifting, which leads to ring opening in which C≡C terminals are formed. In this process the resulting product having conjugated unsaturated bond structure causes a decrease in the optical band gap.[34]

The optical band gap value of the implanted films may be used to characterize their short- and medium-range order. In particular, sizes of graphite-like (sp^2 bonded) regions may be estimated. This issue has been reported in detail by Robertson and O'Reilly.[35] They proposed that from the fundamental absorption edge of amorphous carbon, E_g can be correlated by the following equation:

$$E_g = \frac{2\beta}{\sqrt{M}},$$

where M is the number of six-membered rings that constitute the sp^2-bonded fragments; $\beta = -2.9$ eV is a constant, more specifically, is the nearest-neighbor interaction between the π orbitals of six-membered rings. But Fink et al.[36] showed that the Robertson equation underestimates the cluster size in irradiated polymers. Hence, they assumed that the cluster size is like a buckminsterfullerene structure, i.e., C_{60} ring instead of C_6 ring. With this assumption, they formulated the following expression:

$$E_g = \frac{34.3}{\sqrt{N}},$$

where N is the number of carbon atoms per cluster. By using this relation, the number of carbon atoms in the graphitic clusters for irradiated PC was calculated and is shown in

Table 2. Thus, a progressive increase in the average number of carbon atoms per cluster as a function of the ion flux is inferred from the above relation. Therefore, UV-Vis analysis is consistent with the ion beam–induced agglomeration through which the aromatic rings obtain a new stable state. The drastic decrease of E_g from 4.12 eV for pristine PC to a value of 0.81 eV for PC implanted to a dose 5×10^{14} ions cm^{-2} and finally to a value of 0.50 eV at an implantation dose of 3×10^{16} ions cm^{-2} suggests the transformation from separated aromatic rings to a structure similar to graphite (sp^2 bonded). Similar kinds of observations have been reported by other studies also[3,37] for different ion–polymer combinations; however, the decrease in band gap was not as drastic as it is in our case.

The changes observed in the UV spectra directly correspond to those seen in the micro-Raman spectra. Therefore both Raman spectroscopy and UV-Vis spectroscopy indicate the formation of graphite clusters as a result of Ag^+ implantation.

Conclusions

Raman spectroscopy and UV-Vis spectroscopy show significant modification in the optical and structural properties of PC samples implanted with Ag ions. The disappearance of the characteristic peaks of PC in the Raman spectra of Ag-implanted PC implies that the chemical structure of PC changed completely. The analysis of UV-Vis studies indicate that the optical band gap of PC was reduced drastically from a value of 4.12 eV (unimplanted) to a value of 0.50 eV due to 1 MeV Ag^+ ion implantation at a fluence of 3×10^{16} ions cm^{-2}. Further, the structural characterization using Raman spectroscopy, GXRD, and UV-Vis spectroscopy clearly point toward the formation of carbonaceous graphite-like layer containing a network of graphitic clusters. The sharp decline in band gap is the consequence of the structural changes observed in the PC matrix as a result of silver implantation.

Acknowledgments

The authors are thankful to Department of Science and Technology (DST), New Delhi, India, and UGC-DAE Consortium for Scientific Research, Mumbai Centre, Bhabha Atomic Research Centre, Mumbai, India, for providing kind support. Authors are grateful to Dr. Sanjeev Arora, Department of Chemistry, Kurukshetra University, Kurukshetra, India, for his valuable suggestions in preparing the manuscript. One of the authors (SB) is thankful to Kurukshetra University, Kurukshetra, India, for kind financial support. Authors are also thankful to Mr Arun Kumar, Material Science Division, IGCAR, Kalpakkam, India for his kind help during implantation.

References

1. Wintersgill, M.C. Ion implantation in polymers. Nucl. Instrum. Methods Phys. Res. B **1984**, *1*, 595.
2. Yap, E.; McCulloch, D.G.; McKenzie, D.R.; Swain, M.V.; Wielunski, L.S.; Clissold, R.A. Modification of the mechanical and optical properties of a polycarbonate by 50 keV Ar^+ and H^+ ion implantation. J. Appl. Phys. **1998**, *83*, 3404.
3. Sharma, T.; Aggarwal, S.; Sharma, A.; Kumar, S.; Kanjilal, D.; Deshpande, S.K.; Goyal, P.S. Effect of nitrogen ion implantation on the optical and structural characteristics of CR-39 polymer. J. App. Phys. **2007**, *102*, 063527.
4. Hadjichristov, B.G.; Ivanov, V.; Faulques, E. Reflectivity modification of polymethylmethacrylate by silicon ion implantation. Appl. Surf. Sci. **2008**, *254*, 4820.

5. Wu, Y.; Zhang, T.; Zhang, H.; Zhang, X.; Deng, Z.; Zhou, G. Electrical properties of polymer modified by metal ion implantation. Nucl. Instrum. Methods Phys. Res. B **2000**, *169*, 89.
6. Tavenner, E.; Meredith, P.; Wood, B.; Curry, M.; Giedd, R. Tailored conductivity in ion implanted polyetheretherketone. Synth. Metals **2004**, *145*, 183.
7. Suzuki, Y. Ion beam modification of polymers for the application of medical devices. Nucl. Instrum. Methods. Phys. Res. B **2003**, *206*, 501.
8. Manso, M.; Valsesia, A.; Lejeune, M.; Gilliland, D.; Ceccone, G.; Rossi, F. Tailoring surface properties of biomedical polymers by implantation of Ar and He ions. Acta Biomater. **2005**, *1*, 431.
9. Bhattacharya, R.S. Evaluation of high energy ion-implanted polycarbonate for eyewear applications. Surf. Coat. Technol. **1998**, *103–104*, 151.
10. Zhang, W.; Luo, Y.; Wang, H.; Jiang, J.; Pu, S.; Chu, P. Ag and Ag/N2 plasma modification of polyethylene for the enhancement of antibacterial properties and cell growth/proliferation. Acta Biomater. **2008**, *4*, 2028.
11. Rodríguez, R.J.; Medrano, A.; García, J.A.; Fuentes, G.G.; Martínez, R.; Puertolas, J.A. Improvement of surface mechanical properties of polymers by helium ion implantation. Surf. Coat. Technol. **2007**, *201*, 8146.
12. Rodríguez, R.J.; García, J.A.; Sánchez, R.; Pérez, A.; Garrido, B.; Morante, J. Modification of surface mechanical properties of polycarbonate by ion implantation. Surf. Coat. Technol. **2002**, *158–159*, 636.
13. San, J.; Zhu, B.; Liu, J.; Liu, Z.; Dong, C.; Zhang, Q. Mechanical properties of ion-implanted polycarbonate. Surf. Coat. Technol. **2001**, *138*, 242.
14. Guenther, M.; Gerlach, G.; Suchaneck, G.; Sahre, K.; Eichhorn, K.J.; Wolf, B.; Deineka, A.; Jastrabik, L. Ion-beam induced chemical and structural modification in polymers. Surf. Coat. Technol. **2002**, *158–159*, 108.
15. Valenza, A.; Visco, A.M.; Torrisi, L.; Campo, N. Characterization of ultra-high-molecular-weight polyethylene (UHMWPE) modified by ion implantation. Polymer **2004**, *45*, 1707.
16. Sofield, C.J.; Sugden, S.; Ing, J.; Bridwell, L.B.; Wang, Y.Q. Ion beam modification of polymers. Vacuum **1993**, *44*, 285.
17. Radwan, R.M.; Abdul-Kader, A.M.; El-Hag Ali, A. Ion bombardment induced changes in the optical and electrical properties of polycarbonate. Nucl. Instrum. Methods Phys. Res. B **2008**, *266*, 3588.
18. Stuart, B.H.; Thomas, P.S. Xylene swelling of polycarbonate studied using Fourier transform Raman spectroscopy. Spectrochi. Acta A **1995**, *51*, 2133.
19. Hummel, D.O. (ed.). *Infrared spectra of polymers*. New York: Interscience, 1966, p. 207.
20. Lin-Vien, D.; Colthup, N.B.; Fateley, W.G.; Grasselli, J.G. *The handbook of infrared and Raman characteristic frequencies of organic molecules*. Boston, MA: Academic Press, 1991.
21. Tuinstra, F.; Koenig, J.L. Raman spectrum of graphite. J. Chem. Phys. **1970**, *53*, 1126.
22. Nemanich, R.J.; Solin, S.A. First- and second-order Raman scattering from finite-size crystals of graphite. Phys. Rev. B **1979**, *20*, 392.
23. Chhowalla, M.; Ferrari, A.C.; Robertson, J.; Amaratunga, G.A.J. Evolution of sp^2 bonding with deposition temperature in tetrahedral amorphous carbon studied by Raman spectroscopy. Appl. Phys. Lett. **2000**, *76*, 1419.
24. Robertson, J. Amorphous carbon. Adv. Phys. **1986**, *35*, 315.
25. McCulloch, D.G.; McKenzie, D.R.; Prawer, S.; Merchant, A.R.; Gerstner, E.G.; Kalish, R. Ion beam modification of tetrahedral amorphous carbon: the effect of irradiation temperature. Diamond Relat. Mater. **1997**, *6*, 1622.
26. Ferrari, A.C.; Robertson, J. Interpretation of Raman spectra of disordered and amorphous carbon. Phys. Rev. B **2000**, *61*, 14095.
27. Baptista, D.L.; Zawislak, F.C. Hard and sp^2-rich amorphous carbon structure formed by ion beam irradiation of fullerene, *a*-C and polymeric *a*-C:H films. Diamond Relat. Mater. **2004**, *13*, 1791.
28. Dischler, B.; Bubenzer, A.; Koidl, P. Bonding in hydrogenated hard carbon studied by optical spectroscopy. Solid State Commun. **1983**, *48*, 105.

29. Lee, C.Y.; Kil, J.K. Hydrophilic property by contact angle change of ion implanted polycarbonate. Rev. Sci. Instrum. **2008**, *79*, 02C508.
30. Park, K.J.; Chin, E.Y. Effect of diamond-like carbon thin film deposition on the resistance of polycarbonate to radiation-induced degradation. Polym. Degrad. Stabil. **2000**, *68*, 93.
31. Pavia, D.L.; Lampman, G.M.; Kriz, G.S. *Introduction to spectroscopy*, 2nd ed. New York: Harcourt Brace College Publishers, 1994.
32. Tauc, J.; Grogorovici, R.; Vancu, A. Optical properties and electronic structure of amorphous germanium. Phys. Status Solidi. **1966**, *15*, 627.
33. Zhu, Z.; Sun, Y.; Liu, C.; Liu, J.; Jin, Y. Chemical modifications of polymer films induced by high energy heavy ions. Nucl. Instrum. Methods Phys. Res. B **2002**, *193*, 271.
34. Saravanan, S.; Anantharaman, M.R.; Venkatachalam, S.;. Avasthi, D.K. Studies on the optical band gap and cluster size of the polyaniline thin films irradiated with swift heavy Si ions. Vacuum **2008**, *82*, 56.
35. Robertson, J.; O'Reilly, E.P. Electronic and atomic structure of amorphous carbon. Phys. Rev. B **1984**, *35*, 2946.
36. Fink, D.; Keltt, R.; Chadderton, L.T.; Cardoso, J.; Montiel, R.; Vazquez, H.; Karanovich, A.A. Carbonaceous clusters in irradiated polymers as revealed by small angle X-ray scattering and ESR. Nucl. Instrum. Methods Phys. Res. B **1996**, *111*, 303.
37. Das, A.; Dhara, S.; Patnaik, A. Fractal nature of π-bonded nanocrystalline clusters: A N^+ beam-induced phenomenon in poly(2,6-dimethyl-1,4-phenylene oxide). Phys. Rev. B **1999**, *59*, 11069.